Low-loss terahertz waveguide with InAs-graphene-SiC structure*

Xu De-Gang(徐德刚), Wang Yu-Ye(王与烨)†, Yu Hong(于 红), Li Jia-Qi(李佳起), Li Zhong-Xiao(李忠孝), Yan Chao(闫 超), Zhang Hao(张 昊), Liu Peng-Xiang(刘鹏翔), Zhong Kai(钟 凯), Wang Wei-Peng(王卫鹏), and Yao Jian-Quan(姚建铨)

College of Precision Instrument and Opto-electronics Engineering, Tianjin University, Tianjin 300072, *China*
Key Laboratory of Opto-electronics Information Technology, Tianjin University, Ministry of Education, Tianjin 300072, *China*

(Received 7 August 2013; revised manuscript received 24 October 2013; published online 25 March 2014)

We demonstrate a low-loss terahertz waveguide based on the InAs-graphene-SiC structure. By analyzing the terahertz waveguide proposed in this paper, we can obtain that it is the characteristic of a low transmission loss coefficient ($\alpha_{\rm loss} \approx$ 0.55 dB/m) for fundamental mode ($\rm LP_{01}$) when the incident frequency is larger than 3.0 THz. The critical radii of the inside and outside cylinders have been found for the high-quality transmission. The large inside radius and the high transmission frequency result in a flat transmission loss coefficient curve. As a strictly two-dimensional material, the double graphene surface rings perform better to improve the quality of transmission mode. These results provide a new idea for the research of the long-distance THz waveguide.

Keywords: InAs-graphene-SiC structure, low-loss terahertz waveguide, transmission, critical radii

PACS: 42.65.–k, 61.48.Gh, 42.65.Wi **DOI:** 10.1088/1674-1056/23/5/054210

1. Introduction

With the development of terahertz-wave (THz-wave) research solutions and techniques, the related efficient waveguide propagation of THz-wave essential has attracted considerable interest for the construction of compact THz devices and measurement systems. In order to transport THz wave effectively, many researches have been reported such as bare metal wire, parallel-plate metal waveguide, polymer waveguide, plastic ribbon waveguide, sapphire fiber, and so on.[1–3] However, the design and fabrication of low-loss and broadband waveguide to be used in the terahertz regime is still a challenging research field due to the material absorption and dispersion.

Since the experimental discovery of graphene in 2004, the investigations of graphene-based electronics and optoelectronics have quickly become one of the most important research topics in condensed-matter physics, nanomaterial science, and nanoelectronics. As a two-dimensional lattice of carbon atoms arranged in a honeycomb crystal structure, graphene is a unique material with near-zero band-gap and linear energy–momentum dispersion related to both electrons and holes.[4,5] The unique electronic and optical properties of grapheme, such as the high mobility of electrons ($> 1.5 \times 10^4$ $\rm cm^2{\cdot}V^{-1}{\cdot}s^{-1}$) and high electrical conductivity (10^8 S/m), make it a promising material for the development of high-speed electron devices,[6] and it has been widely applied in telecommunications and waveguide devices. In 2013, He and Kim reported a new structure of Si-SiO_2-graphene-dielectrics-graphene-SiO_2-Si ($SiSiO_2GDGSiO_2Si$) in the terahertz regime by using the finite element method (FEM) and transfer matrix method (TMM). The loss of the $SiSiO_2GDGSiO_2Si$ structure is much smaller compared with other kinds of waveguide structures.[7] In this paper, a low-loss terahertz waveguide based on the InAs-graphene-SiC structure is presented. We discuss the critical radii of the inside (R_1) and outside (R_2) cylinders for the high-quality transmission in this InAs-graphene-SiC structure waveguide. The analysis results show that the InAs-graphene-SiC structure has the characteristic of a low transmission loss coefficient (0.55 dB/m) for the fundamental mode ($\rm LP_{01}$) while $\omega \geq 3$ THz, and the increase of R_1 results in a flat transmission loss coefficient curve. This design provides a new idea for the research of long-distance THz waveguides.

2. Design and theory of terahertz waveguide with InAs-graphene-SiC structure

A graphene-based terahertz waveguide is presented in Fig. 1. The waveguide structure has three parts. InAs is used as the filling material in areas I and III. Area II is filled with a semi-insulating 6H-SiC$\langle 0001 \rangle$ hollow cylinder. The epitaxial graphene samples used in this work are grown on the inside and outside faces of the semi-insulating 6H-

*Project supported by the National Basic Research Program of China (Grant No. 2014CB339802), the National High Technology Research and Development Program of China (Grant No. 2011AA010205), the National Natural Science Foundation of China (Grant Nos. 61107086 and 61172010), the Natural Science Foundation of Tianjin, China (Grant Nos. 11JCYBJC01100 and 13ZCZDSF02300), the Specialized Research Fund for the Doctoral Program of Higher Education of China (Grant No. 20120032110053), and the THz Science and Technology Foundation of China Academy of Engineering Physics (Grant Nos. CAEPTHZ201201 and CAEPTHZ201304).

†Corresponding author. E-mail: yuyewang@tju.edu.cn

© 2014 Chinese Physical Society and IOP Publishing Ltd

SiC⟨0001⟩ hollow cylinder using techniques that have been reported previously.[8] A low-loss terahertz waveguide based on the InAs-graphene-SiC structure is completed.

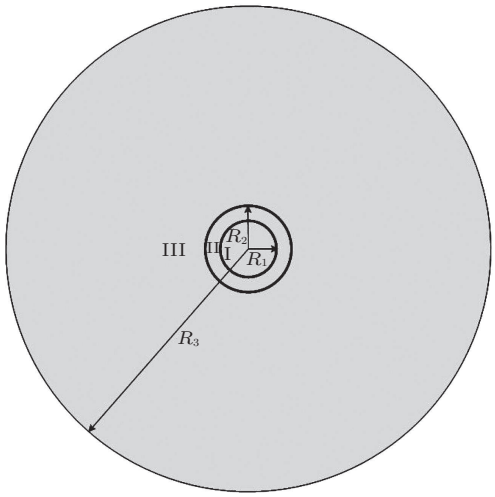


Fig. 1. The structure of graphene-based terahertz waveguide.

It should be noted that the dielectric constant ε_{G} of graphene is 4.0[9] and the electrical conductivity is $\sigma = 10^8$ S/m.[10] The theoretical thickness of a graphene layer is 0.335 nm, we set $d = 1$ nm considering the surface irregularity and the generated oxide layer during the epitaxial growth,[11] and refractive index n_{InAs} varies from 3.12 to 3.52 with the incident wavelengths changing.[12] The distribution of n_{R} for this InAs-graphene-SiC structure is shown in the following equations:

$$n_{\mathrm{R}} = \begin{cases} n_{\mathrm{InAs}}, & (R \le R_1) \cup (R_2 + d < R \le R_3), \\ n_{\mathrm{SiC}}, & R_1 + d < R \le R_2, \\ n_{\mathrm{G}}, & (R_1 < R \le R_1 + d) \cup (R_2 < R \le R_2 + d), \\ n_0, & R > R_3. \end{cases} \tag{1}$$

Here, n_0 and n_{G} are the refractive indices of air and graphene, respectively, and R_1, R_2, and R_3 are the radii of areas I, II, and III, respectively. The thickness of area II ($\Delta R = R_2 - d - R_1$) is about 10 μm, and the simulation result indicates that the varying value of d has little impact on the performance of this waveguide structure in a certain range due to the exceptionally high electrical conductivity of graphene. It can be considered that the double graphene surface rings can limit terahertz waves in the core.

Just like all electromagnetic phenomena, the distribution of an optical field in this structure is governed by Maxwell's equations. For an electromagnetic field with the frequency ω traveling in a nonconducting medium, these equations can be described by the Helmholtz wave equation as[6]

$$\nabla^2 \psi(r, \Phi) + k^2 \psi(r, \Phi) = 0, \tag{2}$$

where $k = \mu_0 \varepsilon_0 \varepsilon_{\mathrm{R}} \omega^2$ is the wave number and $\varepsilon_{\mathrm{R}} = n_{\mathrm{R}}^2$ is the relative dielectric constant, $\mu_0 = 4\pi \times 10^{-7}$ N/A^2 and $\varepsilon_0 = 8.85 \times 10^{-12}$ F/m are the vacuum magnetic permeability and vacuum dielectric constant, respectively. The root of Eq. (2) can be described as $\psi(r, \phi) = R(r) \exp(\pm \mathrm{j} l \phi)$, where $l = 0, 1, 2, \ldots$ This term satisfies the Bessel equation as

$$\frac{\partial^2 R(r)}{\partial r^2} + \frac{1}{r} \frac{\partial R(r)}{\partial r} + \left(k^2 - \beta^2 - \frac{l^2}{r^2} \right) R(r) = 0. \tag{3}$$

From the Bessel differential equation, a canonical solution using a Bessel function of the first kind $\mathrm{J}_\alpha(r)$ and a Bessel function of the second kind $\mathrm{Y}_\alpha(r)$ can be obtained as

$$R(r) = c_1 \mathrm{J}_\alpha(r) + c_2 \mathrm{Y}_a(r). \tag{4}$$

Moreover, the Bessel function includes a modified Bessel function of the first kind $\mathrm{I}_\alpha(r)$ and a modified Bessel function of the second kind $\mathrm{K}_\alpha(r)$. The difference between a modified Bessel function and a general Bessel function is that the general Bessel function is oscillating with the real variable changing, while the modified Bessel function is the exponential growth or exponential damping, $\mathrm{I}_\alpha(r)$ is the same as $\mathrm{J}_\alpha(r)$. In the area I ($R < R_1$), combining with the convergence of the Bessel function, we can obtain

$$R(r) = \mathrm{J}_l(k_1 r). \tag{5}$$

In the areas II and III, we can obtain

$$R(r) = A_2 \mathrm{J}_l(k_2 r) + B_2 \mathrm{Y}_l(k_2 r), \tag{6}$$

$$R(r) = A_3 \mathrm{J}_l(k_3 r) + B_3 \mathrm{Y}_l(k_3 r). \tag{7}$$

The root of the Bessel function in graphene is given by

$$R(r) = C_1 \mathrm{I}_l(k_{\mathrm{G}} r) + D_1 \mathrm{K}_l(k_{\mathrm{G}} r), \tag{8}$$

$$R(r) = C_2 \mathrm{I}_l(k_{\mathrm{G}} r) + D_2 \mathrm{K}_l(k_{\mathrm{G}} r). \tag{9}$$

Here, k_1, k_2, k_3, k_{G} are the wave numbers, which are corresponding to different refractive indices and $k_1 = k_3$ as well. Without an electromagnetic wave revealing outside the waveguide, we take into account $R(r) = 0$.

From electric field continuum boundary, we can obtain

$$\begin{cases} \mathrm{J}_l(k_1 R_1) = C_1 \mathrm{I}_l(k_{\mathrm{G}} R_1) + D_1 \mathrm{K}_l(k_{\mathrm{G}} R_1), \\ C_1 \mathrm{I}_l(k_{\mathrm{G}}(R_1 + d)) + D_1 \mathrm{K}_l(k_{\mathrm{G}}(R_1 + d)) \\ \quad = A_2 \mathrm{J}_l(k_2(R_1 + d)) + B_2 \mathrm{Y}_l(k_2(R_1 + d)), \\ A_2 \mathrm{J}_l(k_2 R_2) + B_2 \mathrm{Y}_l(k_2 R_2) \\ \quad = C_2 \mathrm{I}_l(k_{\mathrm{G}} R_2) + D_2 \mathrm{K}_l(k_{\mathrm{G}} R_2), \\ C_2 \mathrm{I}_l(k_{\mathrm{G}}(R_2 + d)) + D_2 \mathrm{K}_l(k_{\mathrm{G}}(R_2 + d)) \\ \quad = A_3 \mathrm{J}_l(k_3(R_2 + d)) + B_3 \mathrm{Y}_l(k_3(R_2 + d)), \\ A_3 \mathrm{J}_l(k_3 R_3) + B_3 \mathrm{Y}_l(k_3 R_3) = 0. \end{cases} \tag{10}$$

In addition, the continuity of the first-order derivative from the above equations can be known as

$$\begin{cases} \mathrm{J}_l'(k_1R_1) = C_1\mathrm{I}_l'(k_\mathrm{G}R_1) + D_1\mathrm{K}_l'(k_\mathrm{G}R_1), \\ C_1\mathrm{I}_l'(k_\mathrm{G}(R_1+d)) + D_1\mathrm{K}_l'(k_\mathrm{G}(R_1+d)) \\ \quad = A_2\mathrm{J}_l'(k_2(R_1+d)) + B_2\mathrm{Y}_l'(k_2(R_1+d)), \\ A_2\mathrm{J}_l'(k_2R_2) + B_2\mathrm{Y}_l'(k_2R_2) \\ \quad = C_2\mathrm{I}_l'(k_\mathrm{G}R_2) + D_2\mathrm{K}_l'(k_\mathrm{G}R_2), \\ C_2\mathrm{I}_l'(k_\mathrm{G}(R_2+d)) + D_2\mathrm{K}_l'(k_\mathrm{G}(R_2+d)) \\ \quad = A_3\mathrm{J}_l'(k_3(R_2+d)) + B_3\mathrm{Y}_l'(k_3(R_2+d)). \end{cases} \tag{11}$$

3. Simulation of terahertz waveguide with InAs-graphene-SiC structure

Here, we use the finite element method to develop this structural model according to the above waveguide theory. Since the refractive index values of SiC and InAs meet the weakly-guiding approximation, the low order modes will degenerate into LP mode. The two HE_{11} modes degenerate into LP_{01} mode, and TE_{01}, TM_{01}, and HE_{21} degenerate into LP_{11} mode. Figures 2(a) and 2(b) illustrate the intensity distribution of LP_{01} and LP_{11} modes, respectively.

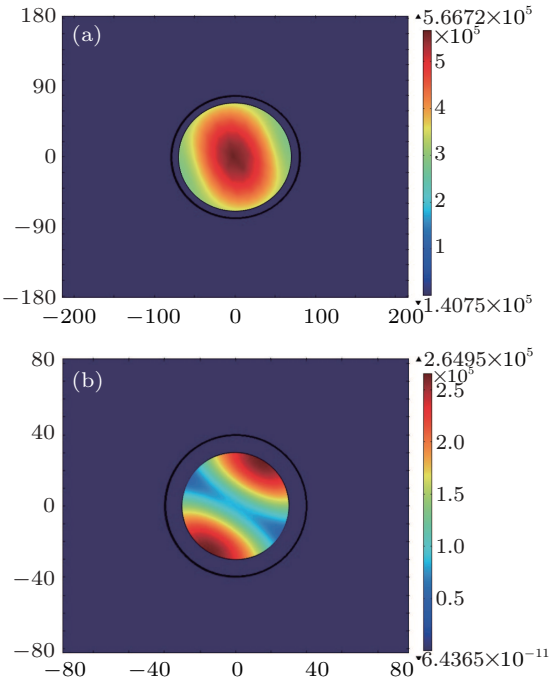


Fig. 2. (color online) The intensity distribution of two different transmission modes: (a) LP_{01} and (b) LP_{11}.

Figure 3 shows the simulating results which illustrate the critical radii of the inside and outside cylinders. In Fig. 3(a), area A represents the transmission mode LP_{01}, and LP_{11} mode would appear when R_1 was chosen in area B. Therefore, we can design the size of R_1 to control a single mode transmission in this waveguide structure. As to the outside radius, the value of R_3 influences the transmission quality directly. The curve in Fig. 3(b) indicates a critical condition. When the value of R_3 is chosen in area C, the polarization orientation of LP_{01} mode is accordant, but the linear polarization would be destroyed while R_3 is chosen in area D.

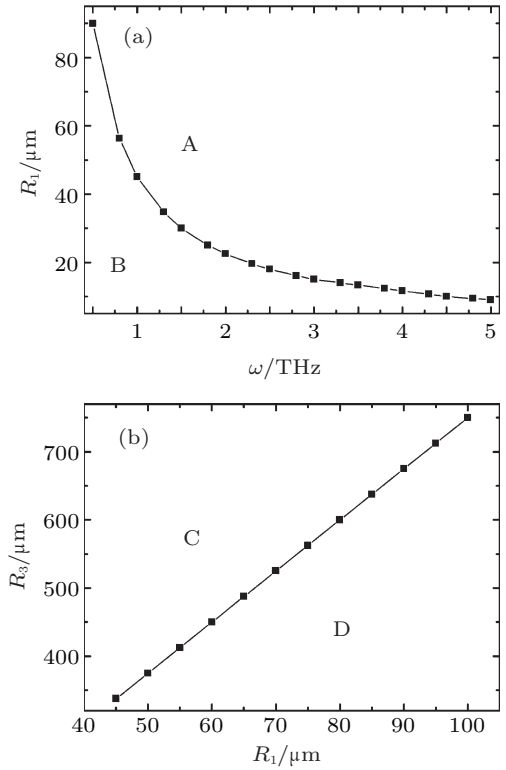


Fig. 3. The critical radii of the inside and outside cylinders. (a) The R_1 as a function of the incident frequency ω, (b) R_3 as a function of the core radius R_1.

In Figs. 4(a)–4(d), the conversion process between two modes is demonstrated under $\omega = 1$ THz. It can be clearly seen that the central intensity drifts to the opposite direction with the decrease of R_1 from 70 μm to 40 μm. The values of 70 μm, 60 μm, 50 μm, and 40 μm for R_1 are chosen as the parameters. The mode has a better polarization state with the increase of R_1. Figure 4(d) illustrates a transition state, so we can control the incident frequency ω and R_1 to obtain LP_{01} mode transmission. An obvious separation trend appears in the mode center. That is to say, the LP_{01} mode would be split into two parts to convert into LP_{11} mode with R_1 decreasing.

As for the mode transmission loss, it is easy to prove that $\alpha = 2k_0\mathrm{Im}(n_\mathrm{eff})$, and α is proportional to $\mathrm{Im}(n_\mathrm{eff})$. When THz wave transmits along with the waveguide, the attenuation of transmission power can be described as follows:

$$P(z) = P_0\,\mathrm{e}^{-\alpha z}. \tag{12}$$

Actually, the transmission loss coefficient α_loss is defined as

$$\alpha_\mathrm{loss} = \frac{10}{Z}\lg\left[\frac{P_0}{P(z)}\right]. \tag{13}$$

Here, Z represents the transmission distance along the z axis, P_0 and $P(z)$ are the powers at $z = 0$ and $z = Z$, respectively. Figure 5 shows the transmission loss coefficient α_loss of the waveguide with the variation of R_1 and ω. The minimum

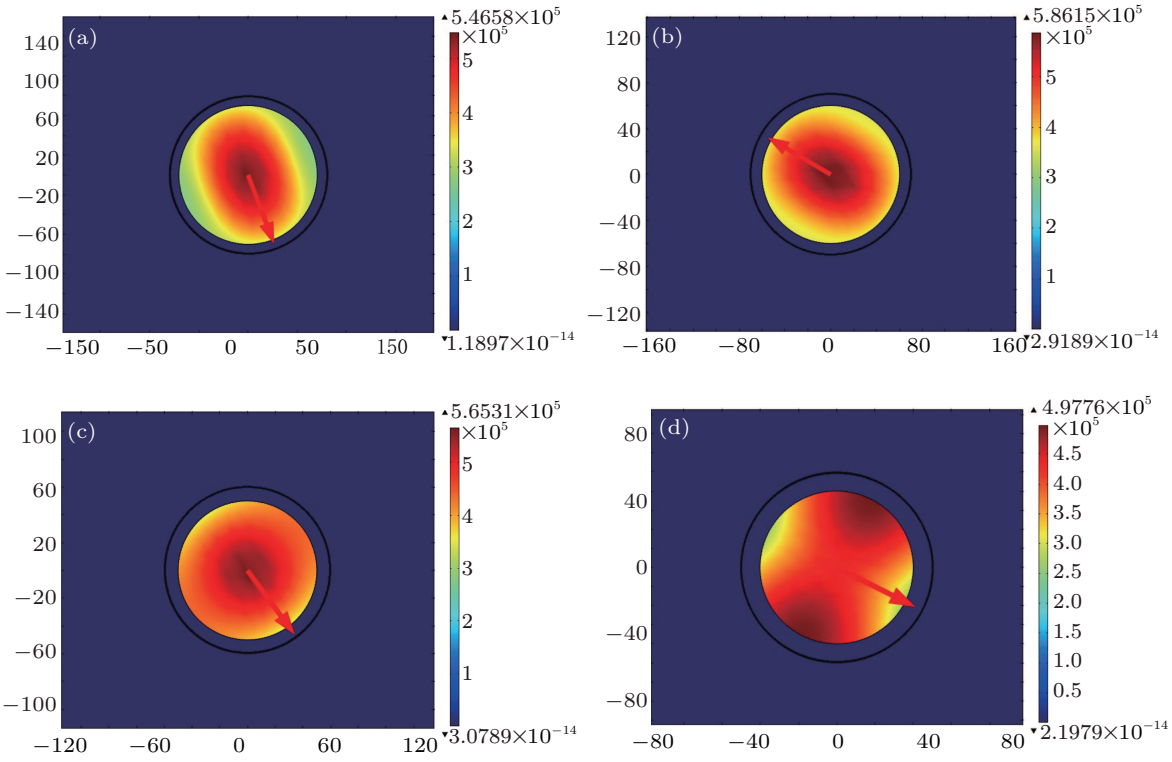


Fig. 4. (color online) One of the linear polarization modes LP_{01} under different inside radii: (a) $R_1 = 70$ μm, (b) $R_1 = 60$ μm, (c) $R_1 = 50$ μm, and (d) $R_1 = 40$ μm.

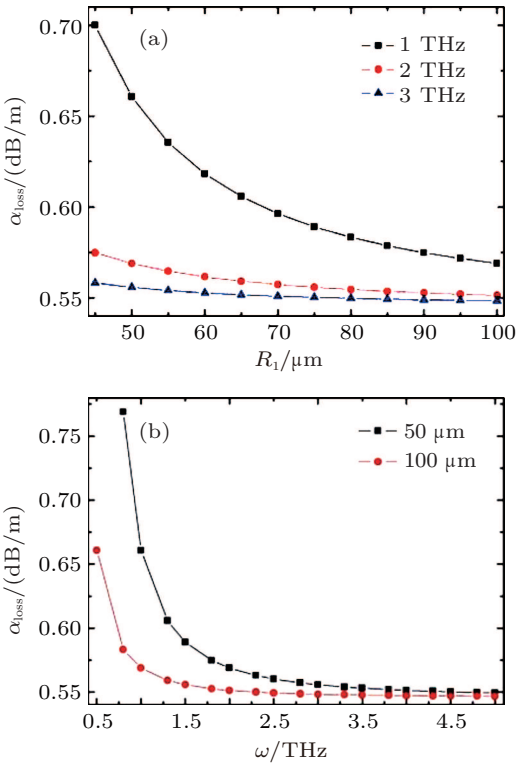


Fig. 5. (color online) The transmission loss coefficient α_{loss} of the waveguide with the variation of (a) R_1 and (b) ω.

of α_{loss} is 0.55 dB/m and it keeps a relatively steady value for $\omega \geq 3$ THz as illustrated in Fig. 5(a). The transmission loss coefficient $\alpha_{loss} = 0.55$ dB/m is an order of magnitude lower than that of the hollow silver waveguide (7–8 dB/m) reported by Ito *et al.* in 2007.[13] Namely, the proposed structure in this paper can be applied for the transmission of THz waves in a long distance. This is mainly because the exceptionally high electrical conductivity of the double graphene surface rings can limit THz waves in the core. Figure 5(b) shows that the larger R_1 leads to a smaller value of α_{loss}, but it has little impact on α_{loss} in the range of higher incident frequencies. That is to say, a relatively large R_1 and high transmission frequency result in a flat transmission loss coefficient curve. Meanwhile, the refractive index of SiC and InAs meet the weakly-guiding approximation.[14] Therefore, this structure can work as a broadband THz waveguide with low transmission loss through rational design of the inside radius.

4. Conclusion

We presented a low-loss terahertz waveguide based on the semiconductor-graphene structure. SiC is chosen as the filler material in area II because of the mature technology for the epitaxial grapheme, and double graphene surface rings perform better in improving the waveguide transmission quality. Critical radii of the inside and outside cylinders have been found and we can obtain the high-quality transmission by controlling the sizes of R_1 and R_3. Analysis results illustrate that the InAs-graphene-SiC structure has the characteristic of a low transmission loss coefficient (0.55 dB/m) for the fundamental mode (LP_{01}) while $\omega \geq 3$ THz. The increasing R_1 results in a flat transmission loss coefficient curve. This provides methods for the broadband terahertz transmission.

References

[1] Hao X, Chen Y F, Wang Z G, Liu J B, He J R and Li Y R 2013 *Chin. Phys. B* **22** 076804

[2] Sun L F, Dong L M, Wu Z F and Fang C 2013 *Chin. Phys. B* **22** 077201

[3] Geng Y F, Tan X L, Wang P and Yao J Q 2008 *Appl. Phys. B* **91** 333

[4] Saito R, Dresselhaus G and Dresselhaus M S 1998 *Physical Properties of Carbon Nanotubes* (London: Imperial College Press) p. 258

[5] Neto A H C, Guinea F, Peres N M R, Novoselov K S and Geim A K 2009 *Rev. Mod. Phys.* **81** 109

[6] George P A, Strait J, Dawlaty J and Shivaraman S 2008 *Nano Lett.* **8** 4248

[7] He X Y and Kim S 2013 *J. Opt. Soc. Am. B* **30** 2461

[8] Dubinov A A, Aleshkin V Y, Maxim R, Taiichi O and Victor R 2009 *Appl. Phys. Express* **2** 092301

[9] Yuan Y Z, Yao J Q and Xu W 2012 *Opt. Lett.* **37** 960

[10] Geim A K and Novoselov K S 2007 *Nat. Mater.* **6** 183

[11] Zhang H, Fu Q, Yi C, Tan D L and Bao X H 2009 *Chin. Sci. Bull.* **54** 2446

[12] Arunachalam N, Peter A J and Yoo C K 2012 *J. Lumin.* **132** 1311

[13] Ito T, Matsuura Y J, Miyagi M, Minamide H and Ito H 2007 *J. Opt. Soc. Am. B* **24** 1230

[14] Gloge D 1971 *Appl. Opt.* **10** 2442